

ANALYTICAL DESCRIPTION OF FRC SUBJECTED TO TRANSIENT LOADS

WOLFGANG WEBER, BERND W. ZASTRAU

Technische Universität Dresden, Dresden, Germany

e-mail: wolfgang.weber@tu-dresden.de

In many real-world applications, such as in civil engineering, non-periodic composite materials are used, whose dynamical behaviour is still not deeply understood, especially concerning its wave scattering properties. In this paper, the scattering of a transient non-plane elastic SH wave by an arbitrary arrangement of identical multi-layered and thus inhomogeneous obstacles is investigated. The obstacles are embedded in a homogeneous, isotropic, and linear elastic matrix of infinite extent. The solution procedure is analytical and will then be evaluated numerically for investigating a small material clipping of a real-world problem.

Key words: random media, multiple scattering, transient loads

1. Introduction

In many engineering applications, the dynamical behaviour of systems or whole structures is of interest. In recent times, materials having certain designated properties have been developed. These include composite materials as they are used in e.g. optics and aerospace engineering. Due to the production process, which takes place under laboratory conditions, these composite materials often are regular even at the microscale, cf. Wächter and Michaelis (2010). This regularity allows both analytical and numerical investigations of a single inclusion within the particular matrix material. Concerning the interaction of the scatterer and the surrounding medium, appropriate mechanical models have to be developed. The single obstacle and the surrounding matrix in its vicinity are then put into a unit- or periodic-cell, where numerous unit-cells represent the whole material aperture, Parnell and Abrahams (2006). For doing this, appropriate boundary conditions between adjacent cells have to be fulfilled, cf. Liu and Su (2010). For combining these unit-cells, several theorems exist, of which the Bloch theorem may be one of the most widespread ones, cf. Datta and Shah (2008). Also, theories dealing with effective (dynamic) properties of periodic media exist. Apparently the first with respect to effective elastic moduli goes back to Voigt (1910), others followed, e.g. Reuß (1929). For problems arising from these theories cf. Achenbach (1973).

On the other hand, particularly in civil engineering some compound materials should have a periodic configuration – but do not have in general. Mainly, these irregularities are induced at the building site, as these new materials are not produced under laboratory conditions, thus giving the main difference to the periodic media mentioned before. One example of a new compound material gaining more and more attention in civil engineering praxis but being produced on-site surely is textile reinforced concrete (TRC), which will shortly be introduced in Section 2. Although some models for evaluating the influence of the aforementioned irregularities exist, these are limited to only a small number of so-called defects, cf. Maurel and Pagneux (2008). Additionally, these are currently restricted to one-dimensional problems. Thus, they are not applicable to the present problem.

In real-life applications, forecasts or simulations concerning the dynamic behaviour of compound materials are made complicated by the fact that both the material and geometrical

properties of the structure and its constituents as well as the dynamic loads themselves may vary, see the experimental investigations in Hummeltenberg *et al.* (2011), for example. Theoretical investigations of such large scale problems will be carried out by means of numerical procedures in most cases. These strategies often involve homogenization techniques including their efficient numerical implementation. For recent developments see e.g. Parnell and Weber (2010). However, in order to adequately describe the dynamic behaviour of a homogenized material, profound insight into its behaviour at the micro- and meso-scale is necessary. As could be shown in e.g. Weber and Zastrau (2009), the scattering behaviour of elastic SH waves depends on the cross section of the respective single scatterer. Additionally, a layered build-up of the reinforcement element does influence the scattering behaviour, too, see also Weber and Zastrau (2009). Experimental investigations showed that the layered built-up of reinforcement elements often includes eccentricities. This was the motivation for the investigations in Weber and Zastrau (2011). The aforementioned contributions thus allow a precise description of the (SH) wave scattering behaviour of a reinforcement element of several cross sections and setups.

What is still missing is the embedding of this analytical method in a framework allowing the investigation of the wave scattering behaviour of an arrangement of several reinforcement elements. Hence, in this paper the wave scattering behaviour of an arbitrary number of inhomogeneous inclusions in a homogeneous linear elastic and isotropic matrix is analyzed. Hereby the scatterers are modelled as double-layered obstacles, whereas both layers are concentric with respect to each other. For this, additional motivations are given in Section 2. Afterwards, the scattering of shear waves by means of a single scatterer is investigated in Section 3 by an analytical approach using time-harmonic waves. The extension to multiple scattering, that is, for dealing with an arbitrary number of scatterers, which allows further analyses especially concerning the interaction of these scatterers with each other, is given in Section 4. So far, the investigations are based on time-harmonic waves, the numerical example given in Section 6 deals with transient loads. The missing link is provided by Section 5, where the Fourier integral is introduced and adapted to the needs within this contribution. In Section 6, all results obtained so far are put together to numerically evaluate a small real-world example. Special focus is set on the interactions of the several inclusions with each other and the embedding matrix. Finally, a conclusion and future tasks are given in Section 7.

2. Textile reinforced concrete

As motivated in Section 1, the scattering of waves is of interest in many areas of engineering. We will focus on civil engineering and herein especially on textile reinforced concrete (TRC), a material having a non-periodic structure due to its production process on-site.

TRC is a new construction material developed particularly to fit the needs of civil engineering praxis. It consists of a fine-grained concrete matrix with a maximum grain size of approx. 0.6 mm and fibres made of glass or carbon which are looped to uni- or multi-axial reinforcement clutches and then are worked into the fine-grained concrete matrix, cf. Schladitz *et al.* (2011). Hence, the rovings of TRC allow a well-directed reinforcement matching the respective load cases as examined in Ortlepp *et al.* (2011), thus giving the main difference to fibre reinforced concrete, that is, a concrete matrix with arbitrarily orientated short fibres of steel, glass, or synthetics. These rovings, which are often called fibres as well, consist of 800 up to 2000 filaments, each with a diameter of approx. 13.5 μm . A view in the direction of the fibres as shown in Fig. 1 gives rise to the assumption that the single filaments do participate differently in the load bearing behaviour. In detail, outer filaments have a better interconnection to the surrounding matrix than the inner ones, cf. Scheffler *et al.* (2009). For some models concerning the decreasing degree of bonding see Lepenies (2007). The glass or carbon fibres and their specific bond behaviour

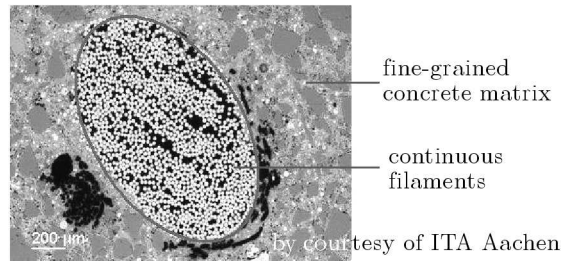


Fig. 1. Setup of a roving with elliptical cross section as discussed in Weber and Zastra (2009)

ensure an improved ductility at least for static load cases. Also, TRC has a high strength. Hence, slender structures as plates show (i) an increased load bearing capacity and (ii) higher deflections than conventionally reinforced structures, see also Fig. 2. The former mentioned properties clearly are an improvement concerning civil engineering applications. The latter has the advantage of announcing critical exposures which may lead to collapse if further increased. With the conventional concrete, the failure is more or less abrupt due to the quasi brittle behaviour of this construction material. With the sponsorship of the German Science Foundation, the static behaviour of TRC was thoroughly investigated within the two Collaborative Research Centres SFB 528 and SFB 532, see e.g. Schladitz *et al.* (2011). However, the dynamic behaviour of TRC is still not understood completely, and so is its behaviour concerning the scattering of waves.

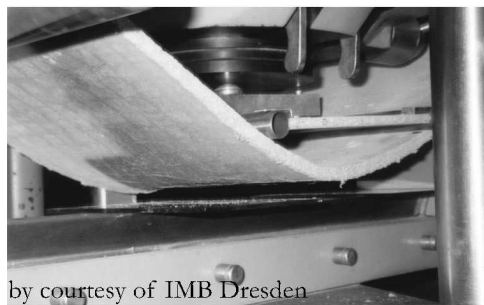


Fig. 2. Quasi-ductile behaviour of TRC

3. Wave scattering by a single inhomogeneous obstacle

The specific build-up of TRC accounts for the investigations within this contribution. Hence, an appropriate mechanical model has to be developed which fits the needs occurring with the given task. As introduced in Section 2, TRC is a composite material made of fine-grained concrete and reinforced with glass or carbon fibres. Due to the radially stratified structure of these rovings, which is due to a decreasing degree of bonding between the filaments constituting the fibres, they are modelled as multi-layered and thus inhomogeneous concentric circular inclusions. Additionally, the matrix behaviour in the vicinity of the rovings will differ from the undisturbed matrix which may be a motivation for introducing an additional layer, commonly known as the interphase, cf. Scheffler *et al.* (2009). For showing the general approach, it is sufficient to model the single roving – which acts as an obstacle for the incoming (non-plane) wave and thus will scatter it – as a double-layered scatterer. The extension to a multi-layered obstacle is straight forward. Herein the inner layer is the roving corresponding to the inner filaments, the outer layer is motivated by the interphase between the outer filaments and the matrix in the vicinity of the fibre. When dealing with other materials, e.g. mortar and steel fibres, this zone is also called interfacial transition zone. As mentioned before, the focus in this contribution is set on

concentric scatterers. For the behaviour of an eccentric scatterer see e.g. Weber and Zastrau (2011). As the concentric scatterer is a special case of an eccentric scatterer, we will restrict ourselves to the basic equations in what follows.

The so-called Navier's equation under absence of (time-dependent) body forces reads as

$$\mu\Delta\mathbf{u} + (\lambda + \mu)\nabla\nabla\cdot\mathbf{u} = \rho\ddot{\mathbf{u}} \quad (3.1)$$

with $\Delta = \nabla^2$, $\mathbf{u} = [u, v, w]^T$ displacement vector, λ , μ Lamé constants and ρ density of the material at hand. It is valid both for pressure (P) and shear (S) waves. For a detailed description of these wave types see e.g. Graff (1991).

In the next Sections, a SH wave is being looked at. Hereby, a polarization is assumed such that the particle motion is parallel to the axis of the matrix inclusion, whose properties do not change along its axis as shown in Fig. 3a. A concentric layered elastic circular cylinder which is embedded in a linear elastic and isotropic medium of infinite extent as depicted in Figs. 3a,b, is thus considered.

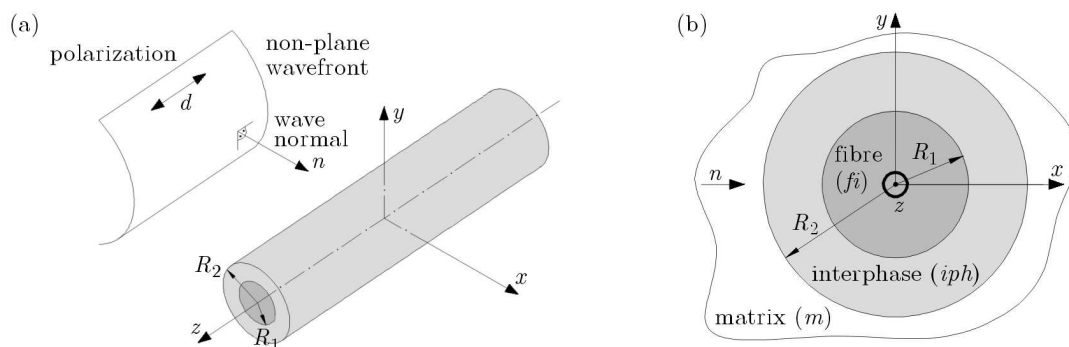


Fig. 3. Problem configuration, concentric circular cylinder case; (a) 3D-view, (b) 2D-view

The resulting waves are sought due to the acting of a time-harmonic incident SH wave. The only nontrivial displacement component for a SH wave scattering problem is the out of plane displacement w , if the SH wave propagates in the xy -plane and the axis of the obstacle is parallel to the z -axis as shown in Fig. 3a. Hence, a time-harmonic ansatz also for the displacement is advantageous. Additionally, a so-called complex amplitude ϕ is introduced. Its absolute value gives the amplitude of the displacement w , whereas its real part gives the displacement at a certain time instance, Graff (1991). Introducing this ansatz into Navier's equation (3.1) yields the Helmholtz equation

$$\Delta\phi + \frac{\omega^2}{c_T^2}\phi = 0 = \Delta\phi + k^2\phi \quad (3.2)$$

Herein the wave number k was introduced.

In order to calculate the waves in the matrix, the interphase and the fibre, the solution to the Helmholtz equation in a circular coordinate system is sought. Using the Laplacian in this coordinate system and the ansatz $\phi(r, \theta) = R(r)\Theta(\theta)$, which separates the radial and the angular part of the solution, two differential equations are obtained, cf. Morse and Feshbach (1953). The solution to the Helmholtz equation in polar coordinates is a linear combination of cylindrical wave functions consisting of simple harmonics as the angular factor and Bessel functions of various kinds as the radial factor

$$R_n(r) = b_{1n}J_n(kr) + ib_{2n}Y_n(kr) = c_{3n}H_n^{(1)}(kr) + c_{4n}H_n^{(2)}(kr) \quad (3.3)$$

cf. Weyrich (1937). Herein $H_n^{(1),(2)}(kr) = J_n(kr) \pm iY_n(kr)$ are the Hankel functions of the first and second kind, respectively. With the time-dependency $\exp(-i\omega t)$ used in this contribution

and the well-known asymptotic expressions of the Hankel functions according to e.g. Weyrich (1937), Harrington (2001), it is

$$\begin{aligned}\exp(-i\omega t)H_n^{(1)}(k_m r) &\sim \sqrt{\frac{2}{\pi k_m r}} \exp\left[i\left(k_m r - \frac{\pi}{4} - n\frac{\pi}{2} - \omega t\right)\right] [1 - \mathcal{O}(r^{-1})] \\ \exp(-i\omega t)H_n^{(2)}(k_m r) &\sim \sqrt{\frac{2}{\pi k_m r}} \exp\left[i\left(-k_m r + \frac{\pi}{4} + n\frac{\pi}{2} - \omega t\right)\right] [1 + \mathcal{O}(r^{-1})]\end{aligned}\quad (3.4)$$

Thus, waves moving outward are represented by Hankel functions of the first kind $H_n^{(1)}(kr)$. For a more detailed description of Bessel- and Hankel functions see Weyrich (1937). Herein and with other parameters the subscripts m , iph , and fi hold with the matrix, the interphase and the fibre, respectively.

The treatment of the single roving as a layered inclusion (and hence as a scatterer for the impinging waves) was motivated in Sections 1 and 2. Based on this, radially stratified configuration ansatz functions have to be derived now. They are composed of wave basis functions describing the general behaviour of the respective waves and wave expansion coefficients which scale the contribution of each basis function. For a detailed discussion of the respective ansatz function(s) within each material involved in the wave scattering process one is referred to e.g. Graff (1991), Cai (2004). In Section 6 we will focus on a transient wave propagating through an arbitrary arrangement of identical but inhomogeneous scatterers. As only the waves in the matrix material will be looked at, only the equations describing the wave fields in the matrix are of interest here. In detail, these are ϕ_{in} for the incoming wave and ϕ_{sc} for the scattered one

$$\begin{aligned}\phi_{in}(k_m, r, \theta) &= \sum_{n=-\infty}^{\infty} A_n J_n(k_m r) e^{in\theta} \\ \phi_{sc}(k_m, r, \theta) &= \sum_{n=-\infty}^{\infty} B_n H_n^{(1)}(k_m r) e^{in\theta}\end{aligned}\quad (3.5)$$

However, for determining the wave expansion coefficients A_n and B_n , boundary conditions have to be fulfilled across all interfaces $r = \{R_1, R_2\}$, which also involve the wave fields in the other materials, that is, within all layers of the single scatterer, cf. Weber and Zastrau (2011). This yields a system of equations for each n and each frequency ω .

The entire field outside the scatterer, which will be evaluated in the next section, is expressible as

$$\phi_{ent} = \phi_{in} + \phi_{sc} = \sum_{n=-\infty}^{\infty} [A_n J_n(k_m r) + B_n H_n^{(1)}(k_m r)] e^{in\theta}\quad (3.6)$$

If the single obstacle is not concentric, extensions as shown in Weber and Zastrau (2011) are necessary. By means of a similar procedure, the extension to inclusions of a more general shape, that is, ellipses, is possible and was shown in e.g. Weber and Zastrau (2009).

4. Wave scattering by an arbitrary arrangement of obstacles

In the precedent Section, the scattering of elastic SH waves by a single inhomogeneous obstacle was derived. In most cases, real-world applications involve numerous scatterers, of course. Thus, a proper procedure for using the insights gained from the single-scatterer-case for the solution of more general tasks is needed. As motivated in Section 2, the focus of this contribution is set on aperiodic media which do not allow the use of the concept of periodically arranged unit-

-cells. One of the first – if not the first – approaches to deal with several obstacles goes back to von Ignatowsky (1914), where an infinite grating of rigid obstacles was looked at. Also, concepts involving average values of wave functions due to a couple of obstacles have been suggested, see Foldy (1945). The restriction to isotropic scattering was overcome with e.g. Twersky (1962). The concept of infinite gratings by von Ignatowsky (1914) was put on a more general basis by Waterman (1976). The concept presented there implies that for an arbitrary time t all scatterers i do have a non-vanishing incoming field $\widehat{\phi}_{in,i}$. Thus, this concept is formulated for the steady-state which actually is not a problem as shall be seen in Section 5.

In general, the total wave field in the matrix material consists of the incoming wave and the waves scattered by all N scatterers

$$\phi_{ent} = \phi_{in} + \sum_{i=1}^N \phi_{sc,i}(\widehat{\phi}_{in,i}) \quad (4.1)$$

cf. Waterman (1976). For the special case $N = 1$, equation (3.6) is obtained. Herein, the wave scattered from scatterer i is dependent on all the waves impinging upon this scatterer i . These are the global incoming wave $\phi_{in,i}$ at the scatterer i and the scattered waves of all other $(N - 1)$ scatterers. Thus,

$$\widehat{\phi}_{in,i} = \phi_{in,i} + \sum_{j=1, j \neq i}^N \phi_{sc,j}(\widehat{\phi}_{in,j}) \quad (4.2)$$

Hence, the associated single scatterer solution of each obstacle has to be known. As all scatterers are assumed to be identical, these solutions are identical, too. In fact, the respective solution was presented in Section 3. Within the expressions for the wave fields exemplarily given with equations (3.5), the global coordinate system has to be replaced by the local coordinate system of the scatterer i . Additionally, the wave expansion coefficients A_n of the incoming wave have to be expressed in this local coordinate system as well to take into account different phases of the incoming wave. With reference to equation (4.2), it is necessary to (re-)express the scattered wave of the scatterer j in the local coordinate system of the scatterer i . Thus, coordinate transformations are inevitable, see also Fig. 4. For this purpose, use of the addition theorem of Bessel functions

$$\mathfrak{Z}_n^{(p)}(kr_i)e^{in(\theta_i - \theta_{ij})} = \sum_{m=-\infty}^{\infty} \mathfrak{Z}_{n+m}^{(p)}(kr_j)J_m(kd)e^{in(\theta_{ji} - \theta_j)} \quad (4.3)$$

proved in Meixner and Schaeffe (1954) is made. Herein, $\mathfrak{Z}_n^{(p)}(kr)$ with $p = 1, \dots, 4$ is the Bessel, Neumann or Hankel function of the first or second kind and order n . It is also known as Graf's addition theorem. By means of this addition theorem, the particular two coordinate systems can be converted to each other. Within equation (4.3) the distance between two scatterers i and j is measured by d . The line connecting both scatterers has an angle θ_{ij} in the scatterers i local coordinate system and θ_{ji} in the coordinate system of the scatterer j , respectively. As can be seen from Fig. 4, the same holds with the coordinates of an arbitrary field point \mathcal{P} which are (r_i, θ_i) and (r_j, θ_j) , respectively. With these transformations and the boundary conditions, the wave expansion coefficients of the scattered and refracted waves can be determined. The entire field in the matrix region due to the incoming wave and the scattered waves of all N obstacles then follows from equation (4.1).

The precedent equations for describing the scattering of waves by an arbitrary distribution of N identical inclusions are based on the assumption that the positions of single obstacles are known deterministically. If this is not the case or if the inner structure of each obstacle may vary, more detailed investigations have to be made. One mathematical framework to perform these investigations is the fuzzy analysis. It was applied to the scattering behaviour of a single eccentric obstacle in Weber *et al.* (2013).

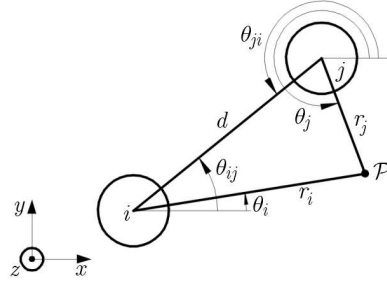


Fig. 4. Definition of the variables for Graf's addition theorem

5. Modelling the transient wave

For given circular frequencies ω , the scattering of time-harmonic elastic SH waves by an arbitrary arrangement of N identical inhomogeneous concentric circular obstacles was derived in the precedent Sections. These steady-state solutions are connected with both the free vibrations and transient responses of the system via the Fourier transform method, cf. Morse and Feshbach (1953). Hence, once the time-harmonic problems are solved by the methods of Sections 3, 4, the propagation of a pulse may be obtained by a Fourier integral.

In general, the load case “pulse” consists of a single principal impulse of an arbitrary shape, which additionally is of a relatively short duration. Although the response of the system to an impulsive load is sought in the time-domain generally, it is often advantageously to perform the respective analyses in the frequency-domain. The investigations of the wave scattering behaviour presented within Sections 3, 4 took place in the frequency-domain on a natural way. Thus, the results obtained so far can be used one by one for the following investigations. The general approach is to (i) express the applied loading in terms of harmonic components, then (ii) evaluate the response of the structure to each of those components (what was done in the precedent Sections), and finally (iii) superpose the harmonic responses to obtain the total structural response, see e.g. Clough and Penzien (1995). Obviously at least the material behaviour at the frequencies dominating the impulse-load has to be known. For real-life applications, this knowledge may be gained from both time-harmonic experiments and frequency analyses of the materials rebound to well-defined short-time exposures under laboratory conditions, see de Andrade Silva *et al.* (2011).

In order to apply the periodic-loading technique to arbitrary loadings the Fourier series concept obviously has to be extended, thus allowing the treatment of non-periodic functions, cf. Clough and Penzien (1995). The clue is to let the period of the load, over which the integration has to take place, go against infinity so that no spurious repetitive loading occurs. In the limit case

$$p(t) = \frac{1}{2\pi} \int_{-\infty}^{\infty} P(\omega) e^{-i\omega t} d\omega \quad P(\omega) = \int_{-\infty}^{\infty} p(t) e^{i\omega t} dt \quad (5.1)$$

is obtained, where the first equation is known as the inverse (exponential) Fourier transform and the latter one as the direct (exponential) Fourier transform, respectively, see also Bronstein *et al.* (2000). Herein, the arbitrary loading $p(t)$ can be expressed as an infinite series of simple harmonics having known complex amplitudes. The complex amplitude again contains information concerning the amplitude and phase of the associated oscillation, see also e.g. Morse and Feshbach (1953).

The necessary conditions for the existence of the direct Fourier transform are given with the Dirichlet-Jordan criteria, one of which is that the integral

$$\int_{-\infty}^{\infty} |p(t)| dt < \infty \quad (5.2)$$

is finite – which clearly is the case if the loading $p(t)$ has a finite duration. Concerning the modulated signal, several waveforms are applied in engineering praxis. For some pulse shapes that are used in Structural Health Monitoring see Schulte (2011), Hennings and Lammering (2010). For these practical applications, the infinite (exponential) Fourier transforms have to be expressed in their approximate finite forms.

6. Numerical example

In the following, the scattering of a SH pulse by an arbitrary arrangement of identical elastic circular concentric obstacles is evaluated by means of the insights of the precedent sections. As the focus is set on the interaction of the scatterers, a plane SH wave is applied. For a plane wave, the wave expansion coefficients A_n as introduced with equation (3.5)₁ follow from the Jacobi-Anger expansion to $A_n = i^n$. The material parameters forming the basis for the calculations presented here are given with Table 1 and were taken from SFB 528. Concerning the number of obstacles, $N = 3$ was chosen to maintain a small example allowing basic insights.

Table 1. Material properties of a certain type of TRC

| Constituent | Matrix | Carbon fibre | Interphase |
|-----------------------------|--------|--------------|------------|
| ρ [kg/m ³] | 2 160 | 1 760 | 1 500 |
| μ [GPa] | 12 | 97 | 1.17 |
| ν [-] | 0.2 | 0.0 | 0.49 |
| c_T [m/s] | 2 340 | 7 440 | 880 |

The transient load was chosen as

$$p(t) = \int_0^{2\omega_0} \sin^2\left(\frac{\pi\omega}{2\omega_0}\right) w(\omega) e^{-i\omega t} d\omega \quad (6.1)$$

which gives rather distinct pulses and uses as much as possible of the computed data from the frequency-domain according to Boström *et al.* (1994). The corresponding signal in the time-domain is plotted in Fig. 5a and is quite similar to a sinc-pulse, the frequency spectrum of the transient load is plotted in Fig. 5b.

The plane SH pulse impinging upon the surface of the arrangement of scatterers has unit amplitude and propagates in the positive x -direction as can be seen from Fig. 6. The $N = 3$ identical elastic circular concentric scatterers of radius $R_2 = 1$ are located at

$$\hat{\mathbf{x}}_{scatterers} = \{(-5, -5), (0, 5), (5, 0)\} \quad (6.2)$$

wherein normalization with the wavelength $\lambda_0 = 2\pi c_T/\omega_0$ connected with the mid-frequency ω_0 of equation (6.1) was applied. Figure 6a shows the geometry of the problem at hand at the time instant $\tau = 2$. Herewith, τ is a dimensionless time given with

$$\tau = \frac{c_T}{R_2} t \quad (6.3)$$

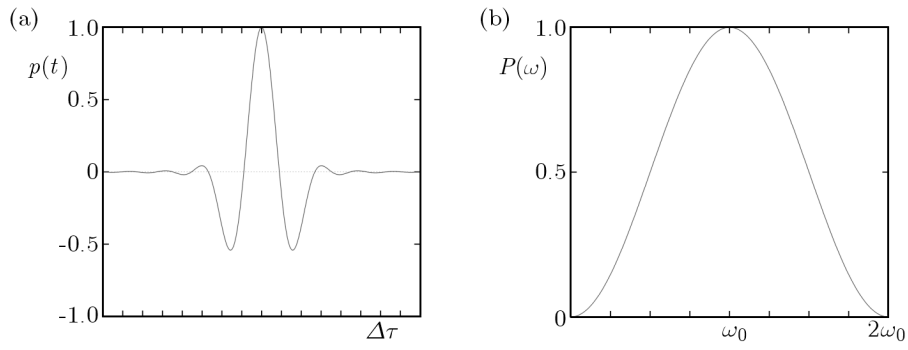


Fig. 5. (a) Applied pulse (Boström-pulse) in the time-domain; (b) frequency spectrum of the applied pulse

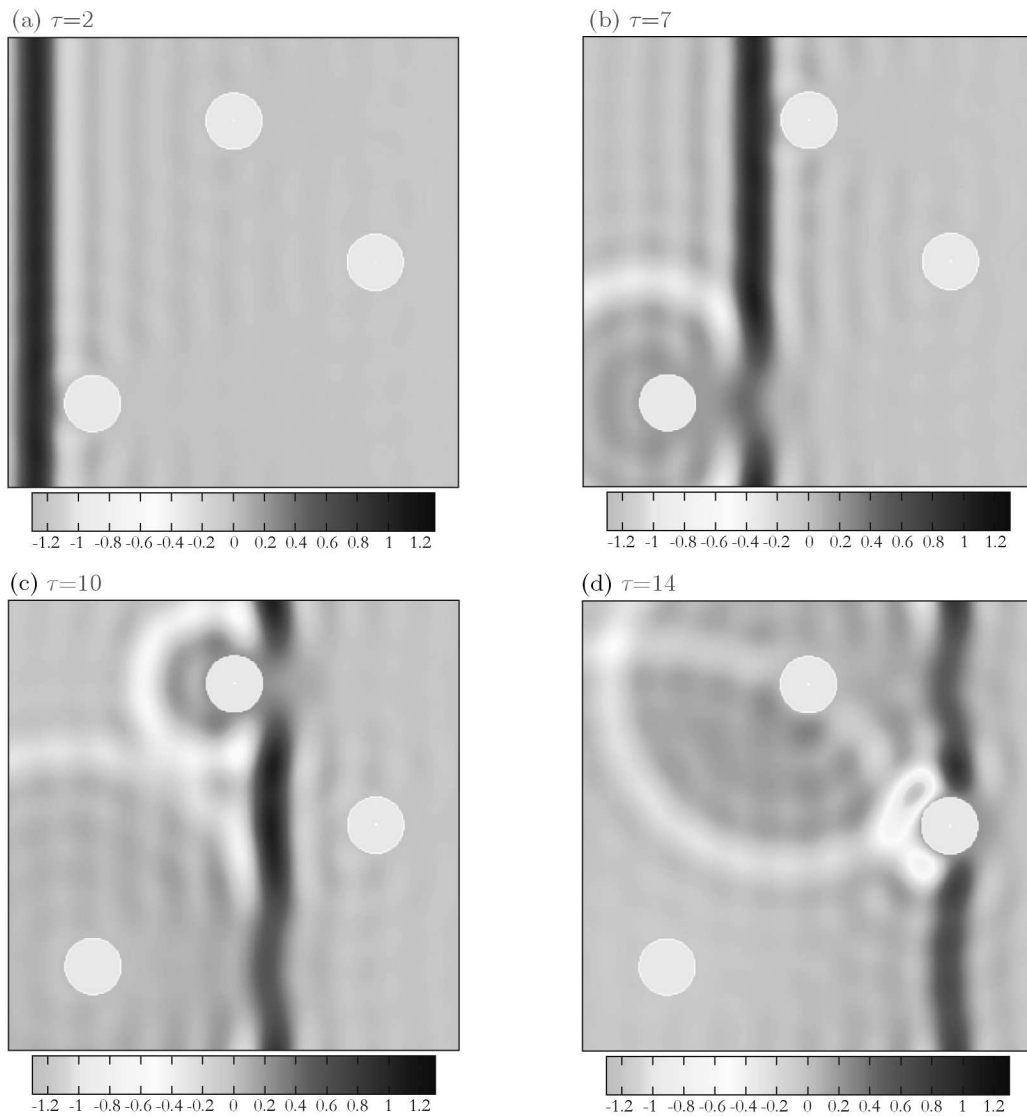


Fig. 6. ϕ_{ent} due to a pulse for different dimensionless times $\tau = (c_T/R_2)t$

With respect to the forthcoming analyses it is advantageous to enumerate the obstacles. In this respect, the sequence follows the arrival time of the pulse, see equation (6.2).

Within Fig. 6, the contour plots of the displacement field for various values of τ are shown. The pulse is applied at $\tau = 0$ at the left hand side of the plot. At $\tau = 2$, the so-far undisturbed

pulse impinges upon the surface of the 1st obstacle thus inducing both a reflected and refracted wave. As can be seen from Fig. 6b, at $\tau = 7$ the reflected wave radially moves outward. On the other hand, the former undisturbed pulse has a decreased amplitude within the shadow region of scatterer 1. The current time instant $\tau = 7$ is also characterized by the impinging of the impulsive load upon the surface of scatterer 2. The reflected wave of scatterer 2 can clearly be identified from Fig. 6c at $\tau = 10$. It is also apparent that the reflected wave of scatterer 1 radially moves outward further, thus decreasing its amplitude due to energy conservation. In the next Fig. 6d, the weakened pulse has already met scatterer 3 at $\tau = 14$. Please note the remarkable interference of the reflected waves of scatterers 1, 2, and 3 directly in front of the 3rd scatterer leading to exposures exceeding the one of the incoming pulse enormously. If the incident wave leads to exposures comparable to the strength of the material, these interference effects could induce cracks and hence could cause a local failure.

7. Conclusion

The derived analytical approach is capable of investigating wave scattering problems as they arise in e.g. civil engineering, mechanical engineering and related disciplines. It allows arbitrary positioning of the single obstacles. Hence, the method is applicable in particular to materials produced on-site. As no meshing and other time-consuming procedures are required for numerical investigations, this approach is very efficient and may be – for special cases – an addendum or even an alternative to numerical methods such as FEM or XFEM. Thus, the approach given here allows in-depth analyses of composite materials such as TRC, which lead to deeper insights into the material behaviour at the micro- and meso-scale. By means of these insights, proper mechanical models allowing efficient simulations at the macro- or structural-scale may be derived.

With engineering structures, impulsive loads are events occurring seldomly, thus giving respective security margins with respect to the strength of the chosen material. On the other hand, the numerical example within this contribution showed that within the scattering process of waves arising from impulsive loads the already huge exposures to the material at hand may even be further increased due to the interference of the incoming and scattered waves. Hence, a detailed investigation of the material is vital. The proposed method also allows substantiated forecasts concerning testing of both damaged and undamaged materials. These forecasts are necessary to evaluate the measuring results obtained from non-destructive testing (NDT) and the monitoring data from non-destructive evaluation (NDE) processes, e.g. in Structural Health Monitoring. Concerning the investigation of damaged structures, the voids/cracks are modelled as circular cavities, see Deng and Yang (2011). These cavities are degenerated cases of the inhomogeneous elastic obstacles dealt with here, cf. Weber and Zastrau (2009).

Future investigations are necessary to allow predictions concerning the wave scattering behaviour of an arbitrary number of different inclusions. These different inclusions may be caused by chemical processes within concrete hardening which may additionally lead to eccentricities within the fibre and the surrounding interphase. Also, focus was set on SH waves so far. Hence, the scattering of both SV and P waves by arbitrary reinforcement arrangements has to be studied in the future.

References

1. ACHENBACH J.D., 1973, *A Theory of Elasticity with Microstructure for Directionally Reinforced Composites*, Springer Verlag, Wien, New York
2. BOSTRÖM A., JOHANSSON M., SVEDBERG T., 1994, Elastic wave propagation in a radially anisotropic medium, *Geophysical Journal International*, **118**, 2, 401-410

3. BRONSTEIN I.N., SEMENDJAJEW K.A., MUSIOL G., MÜHLIG H., 2008, *Taschenbuch der mathematik*, Harri Deutsch Verlag, Frankfurt am Main
4. CAI L.W., 2004, Multiple scattering in single scatterers, *Journal of the Acoustical Society of America*, **115**, 3, 986-995
5. CLOUGH R.W., PENZIEN J., 1995, *Dynamics of Structures*, Computers & Structures Inc., Berkeley
6. DATTA S.K., SHAH A.H., 2008, *Elastic Waves in Composite Media and Structures – with Applications to Ultrasonic Nondestructive Evaluation*, CRC Press, Inc., Boca Raton.
7. DE ANDRADE SILVA F., BUTLER M., MECHTCHERINE V., ZHU D., 2011, Strain rate effect on the tensile behaviour of textile-reinforced concrete under static and dynamic loading, *Materials Science and Engineering: A*, **528**, 3, 1727–1734
8. DENG Q.T., YANG Z.C., 2011, Scattering of s0 lamb mode in plate with multiple damage, *Applied Mathematical Modelling*, **35**, 1, 550-562
9. FOLDY L.L., 1945, The multiple scattering of waves. I. General theory of isotropic scattering by randomly distributed scatterers, *Physical Review*, **67**, 3/4, 107-119
10. GRAFF K.F., 1991, *Wave Motion in Elastic Solids*, Oxford University Press, Oxford
11. HARRINGTON R.F., 2001, *Time-Harmonic Electromagnetic Fields*, Wiley & Sons, New York
12. HENNINGS B., LAMMERING R., 2010, Modelling of wave propagation using spectral finite elements, *PAMM*, **10**, 1, 7-10
13. HUMMELTENBERG A., BECKMANN B., WEBER T., CURBACH M., 2011, Betonplatten unter stoßbelastung – fallturmversuche, *Beton-und Stahlbetonbau*, **106**, 3, 160-168
14. LEPENIES I., 2007, *Zur hierarchischen und simultanen multi-skalen-analyse von textilbeton*, Institut für Mechanik und Flächentragwerke, Technische Universität Dresden, Dresden
15. LIU W., SU X., 2010, Collimation and enhancement of elastic transverse waves in two-dimensional solid phononic crystals, *Physics Letters A*, **374**, 29, 2968-2971
16. MAUREL A., PAGNEUX V., 2008, Effective propagation in a perturbed periodic structure, *Physical Review B*, **78**, 5, 052301
17. MEIXNER J., SCHAEFKE F.W., 1954, *Mathieusche funktionen und sphäroidfunktionen*, Springer Verlag, Heidelberg
18. MORSE P.M., FESHBACH H., 1953, *Methods of Theoretical Physics*, McGraw-Hill, New York
19. ORTLEPP R., SCHLADITZ F., CURBACH M., 2011, Textilbetonverstärkte stahlbetonstützen, *Beton-und Stahlbetonbau*, **106**, 9, 640-648
20. PARNELL W., ABRAHAMS I.D., 2006, Multiple scattering in periodic and random media: An overview, *Proceedings of the GDR 2051 Conference*, 92-99
21. PARNELL W., WEBER W., 2010, Symposium on wave scattering with applications, *AIP Conference Proceedings*, **1281**, 1, 1740-1740
22. REUSS A., 1929, Berechnung der fließgrenze von mischkristallen aufgrund der plastizitätsbedingung für einkristalle, *ZAMM*, **9**, 1, 49-58
23. SCHEFFLER C., GAO S., PLONKA R., MÄDER E., HEMPEL S., BUTLER M., MECHTCHERINE V., 2009, Interphase modification of alkali-resistant glass fibres and carbon fibres for textile reinforced concrete. II Water adsorption and composite interphases, *Composites Science and Technology*, **69**, 7/8, 905-912
24. SCHLADITZ F., LORENZ E., CURBACH M., 2011, Biegetragfähigkeit von textilbetonverstärkten stahlbetonplatten, *Beton- und Stahlbetonbau*, **106**, 6, 377-384
25. SCHULTE R.T., 2011, *Modellierung und simulation von wellenbasierten structural-health-monitoring-systemen mit der spektral-elemente-methode*, Institut für Mechanik und Regelungstechnik – Mechatronik, Universität Siegen, Siegen

26. TWERSKY V., 1962, On scattering of waves by the infinite grating of circular cylinders, *IEEE Transactions on Antennas and Propagation*, **10**, 6, 737-765
27. VOIGT W., 1910, *Lehrbuch der kristallphysik*, Teubner, Leipzig
28. VON IGNATOWSKY W.S., 1914, Zur theorie der gitter, *Annalen der Physik*, **349**, 11, 369-436
29. WATERMAN P.C., 1976, Matrix theory of elastic wave scattering, *Journal of the Acoustical Society of America*, **60**, 3, 567-580
30. WÄCHTER C., MICHAELIS D., 2010, Simulation of metallic nanoparticles in layered structures, *AIP Conference Proceedings*, **1281**, 1, 1626-1629
31. WEBER W., REUTER U., ZASTRAU B.W., 2013, An approach for exploring the dynamical behaviour of inhomogeneous structural inclusions under consideration of epistemic uncertainty, *Multi-discipline Modeling in Materials and Structures*, **9**
32. WEBER W., ZASTRAU B.W., 2009, On sh wave scattering in trc – part I: Concentric elliptical inclusion, *Machine Dynamics Problems*, **33**, 2, 105-118
33. WEBER W., ZASTRAU B.W., 2011, Non-plane wave scattering from a single eccentric circular inclusion – part I: Sh waves, *Journal of Theoretical and Applied Mechanics*, **49**, 4, 1183-1201
34. WEYRICH R., 1937, *Die zylinderfunktionen und ihre anwendungen*, Teubner, Leipzig

Analityczny opis właściwości kompozytów wzmacnianych włóknami poddanych obciążeniom zmiennym

Streszczenie

W rzeczywistych obiektach, np. w inżynierii lądowej, zastosowanie znajdują materiały kompozytowe o strukturze nieperiodycznej. Dynamika takich elementów nadal pozostaje niedostatecznie rozpoznana, zwłaszcza w kontekście właściwości rozpraszania fal. W prezentowanej pracy omówiono problem rozpraszania przejściowych, niepłaskich fal sprężystości spolaryzowanych poziomo (typu SH) w dowolnym układzie identycznych, wielowarstwowych, i przez to niejednorodnych, ekranów tłumiących. Założono, że ekrany te zostały wbudowane w jednorodną, izotropową, liniowo-sprężystą osnowę o nieskończenie wielkich rozmiarach. Zaproponowano analityczne rozwiązanie problemu, które posłuży symulacjom numerycznym efektu słabego obcinania fali w materiale wybranego obiektu rzeczywistego.

Manuscript received January 11, 2012; accepted for print April 23, 2012